JOURNAL OF PROPULSION AND POWER
Vol. 23, No. 5, September–October 2007

Emissive Membrane Ion Thruster Concept

Paul J. Wilbur*
Colorado State University, Fort Collins, Colorado 80523
Merrill Wilson† and Kent Hutchings‡
Ceramatec, Inc., Salt Lake City, Utah, 84119
and
John D. Williams§
Colorado State University, Fort Collins, Colorado 80523

DOI: 10.2514/1.25557

Experiments conducted on solid-state ionic membranes designed to convert atoms into ions that can be extracted into energetic beamlets and thereby produce thrust are described. The processes of ionizing and transporting ions are shown to be both rapid (over 10 $\mathrm{mA/cm^2}$) and efficient (beam ion energy cost on the order of 1 $\mathrm{eV/ion}$). Although similar in appearance to cesium contact sources, solid-state ionic membrane devices are shown to operate successfully at lower temperatures (400 to 700°C). Thus, they have overall efficiencies much greater than those for cesium-based thrusters. The process of extracting the ions by field emission is shown to limit the extracted ion current density. The need to select an emissive surface material/propellant ion combination with a low work function is suggested. Based on successful demonstrations of ion extraction, the emissive membrane ion thruster is proposed. It is shown to offer the potential for substantial reductions in ion thruster system cost and complexity, as well as improvements in scalability and reliability compared with existing ion thrusters.

I. Introduction

THE use of electron-bombardment ion thrusters in space, which began in the United States with the launch of Space Electric Rocket Test 1 (SERT 1) in 1964 [1], has progressed to the point at which over a hundred are now operating on geosynchronous communication satellites. In addition, the highly successful Deep Space 1 mission [2] and thrusters from other countries have shown the usefulness and adaptability of this technology for ambitious high-total-impulse missions in hostile space environments. There is a tendency under such circumstances to seek only marginal thruster improvements through modest design refinements. It is, however, worthwhile to examine recent technological advances to determine if they enable dramatically different designs with markedly improved capabilities for space missions of current interest.

An evolving technology that holds great potential for ion thruster applications is that associated with solid-state ionic conductors [3]. Applications of this technology in everyday life are growing rapidly as a very wide range of new devices evolves. Presently, solid-state ionic conductors are the key elements in the ubiquitous oxygen sensors used in automobile exhaust systems, in lithium ion batteries, in solid oxide fuel cells, in electrochromic windows, and in some superconductors. They are a potentially attractive element for ion thrusters, because they enable the production and delivery of ions to sites at which they can be extracted into a beam without the complications of a plasma discharge chamber and all of its essential components.

This paper presents the results of preliminary experiments designed to investigate the feasibility of using an ionic conductor in the form of a membrane as the element that ionizes neutral propellant molecules and enables their extraction into a collimated energetic ion beam.

II. Basic Physical Model

Although amorphous ionic conductors exist, the typical building block of the membranes used in this study is a crystal similar to the one shown in Fig. 1. As the figure suggests, it contains propellant anions and cations that are bonded chemically. For the case shown, the propellant forms negatively charged anions, but the conductor could be designed to conduct positively charged cations instead. To induce a high ionic conductivity, defects are created in the crystal structure by introducing dopants and/or deviations from stoichiometry. Grain size, membrane density, and purity of starting materials also influence defect formation. In an application, many crystals similar to the one shown in Fig. 1 would be coupled together to form the extensive structure through which ions could be conducted at reasonable current density levels from a region in which they were produced to one in which they would be extracted into beamlets. The overall sequence of events associated with ion membrane operation is shown in Fig. 2. Beginning at the right, an ion is extracted from the anion pool available near the surface of a downstream layer. As ions continue to be extracted, new ones diffuse through the ionic conductor by jumping from one vacancy site to the next, thereby replenishing that pool. These anions are drawn ultimately from a reservoir of propellant molecules adjacent to the ionization layer shown on the left in Fig. 2. The ionization layer, which is porous and in close contact with both the propellant molecules and the ionic conductor, is a good electrical conductor. It is connected to an external current source, and it thereby serves to transfer charge to propellant atoms as they pass through the layer to adjacent vacancies inside the membrane. In so doing, atoms become anions and begin the process of transmission through the ionic conductor. An ion thruster specialist might envision the downstream surface of the membrane as the replacement for the screen hole plasma sheath and the membrane itself as the replacement for the discharge chamber plasma.

It is noted that the diffusion process through the ionic conductor is facilitated by greater temperatures, by favorable electrical potential gradients, and in the case of Fig. 2, by a greater anion density gradient. It is also noted that connection of the downstream layer to

---

Received 1 June 2006; revision received 1 March 2007; accepted for publication 28 May 2007.

*Professor, Department of Mechanical Engineering; pwilbur@engr.colostate.edu. Associate Fellow AIAA.

†Senior Engineer; Wilson@ceramatec.com.

‡Materials Engineer, Solid Electrolyte Oxygen Separation; khutchings@cermatec.com.

§Assistant Professor, Department of Mechanical Engineering; johnw@engr.colostate.edu.

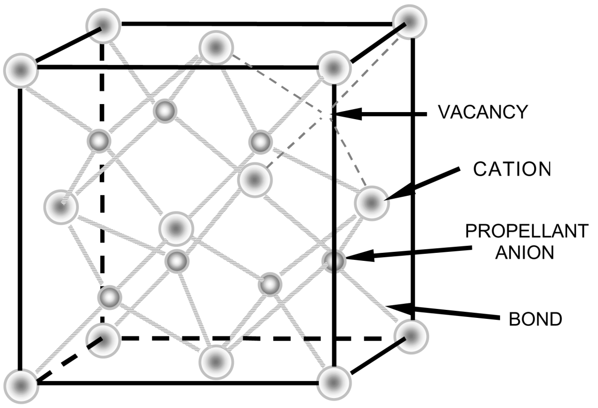

Fig. 1 Typical binary ionic compound structure.

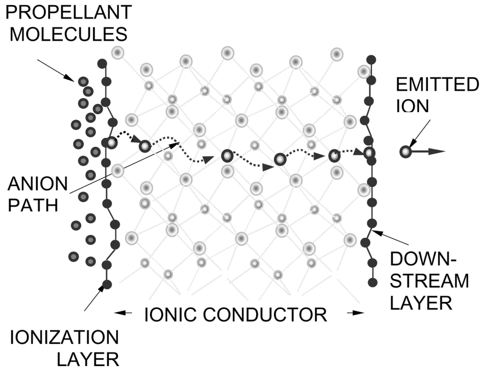

Fig. 2 Membrane process diagram for anion transmission.

the ionization layer via an appropriate external circuit enables electron removal from the anions, thereby generating atoms at the downstream layer. In this case, the atoms can recombine, thereby reforming molecules that flow directly into the downstream vacuum environment, rather than being extracted as anions via an electric field. Such a process would be avoided in a thruster, but it was used in this study to evaluate the ionization and diffusion capabilities of membranes alone (i.e., without the complication of ion extraction).

III. Apparatus and Procedures

To determine if solid-state ionic conductors would be suitable for ion thruster applications, a series of tests designed to identify promising features and potential problems associated with the technology was conducted. The specific tests involved the following:

1) Measurement of the capacity of the membrane (in $\mathrm{mA/cm^2}$) to ionize and then conduct propellant anions through the membrane as a function of its temperature and the voltage difference developed across it.

2) Measurement of the capacity of the membrane to ionize, conduct, and then emit the anions electrostatically from its downstream surface as a function of temperature.

3) Less important effects such as those related to propellant supply pressure.

4) Investigation of the charge state of the anions in the membrane.

Before conducting these tests, it was necessary to select a working fluid and its associated membrane. Solid-state materials have been fabricated to conduct a number of elements, including silver, mercury, oxygen, hydrogen, lithium, lead, and bismuth [3]. Materials proprietary to Ceramatec, Inc. and suitable for use with oxygen were selected because they were available at reasonable cost and could be fabricated into a shape suitable for proof-of-concept testing in a reasonable time. The ceramic membranes fabricated and tested were typically flat discs $\sim$1 mm thick and 0.64 cm in diameter. This active element was mounted in a 2-cm-diam inert ceramic disc of similar thickness, which was then bonded to a stainless steel cup and tube assembly in the manner shown in Fig. 3. The membrane assembly was placed in a cryopumped vacuum chamber maintained in the high 10^{-7} torr range during testing. The cup and tube assembly was supported in the chamber via a vacuum feedthrough. As Fig. 3 suggests, a chromel–alumel thermocouple (T/C) was placed through the tube so that it was in good radiative communication with the membrane and could be used to sense its temperature. A swaged heater wrapped around the cup was used to heat the assembly and maintain its temperature. The oxygen, which flowed from left to right through the membrane during operation (Fig. 3), was also supplied through the tube and its pressure was measured using a Baratron gauge. Preliminary tests showed that the magnitude of this pressure did not affect operation significantly, and because 10 torr yielded a low membrane stress level, this pressure was used throughout the study. The cup and tube assembly and the lines that supplied the oxygen were evacuated and refilled before each test to ensure that gas impurities did not accumulate next to the membrane. The residual gas analyzer (RGA) shown in Fig. 3 had the sensitivity required to measure the partial pressures of recombined oxygen ions that flowed through the membrane during the tests. These partial pressures were converted to oxygen flow rates using a correlation plot generated by feeding oxygen directly into the vacuum chamber and making simultaneous measurements of oxygen flow rate in the mA-equivalent range and oxygen partial pressure.

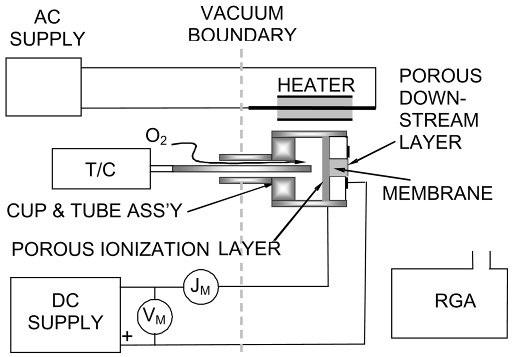

Fig. 3 Membrane flow and current measurement schematic.

The membrane power supply shown in Fig. 3 was used to apply low voltages across the membrane via the conducting layers on its cathode (ionization layer at 10 torr) and anode (downstream layer at high vacuum) sides. This arrangement was used only during the first set of tests, in which the ionization and current-carrying capabilities of the membranes themselves were measured. After these tests were completed, the membrane power supply was removed and a downstream ion extraction (accel) electrode was installed, along with high-voltage power supplies used to apply bias voltages to the cathode and accel electrodes relative to ground. The second series of tests was designed to investigate the combined effects of ion production, ion transmission through the membrane, and ion extraction/acceleration from its downstream surface. The arrangement of the equipment used in these tests is shown schematically in Fig. 4. Also shown is a mass spectrometer that was used to determine the relative currents of the negative ions and electrons that were being

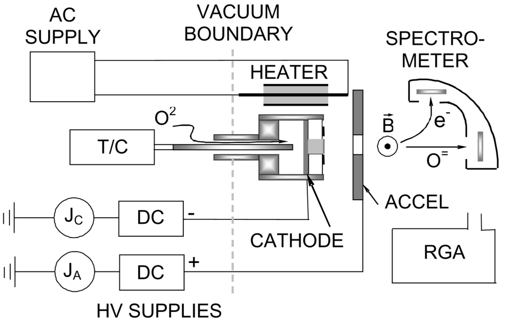

Fig. 4 Schematic of apparatus for ion extraction testing.

extracted. This instrument, which was fabricated specifically for these tests, used a 20-G magnetic field applied normal to the ion beamlet axis. At a nominal net accelerating voltage of 500 V, this magnetic field yielded electron and ion cyclotron radii of 5 cm and 6 m for the electrons and ions, respectively. The currents of these two streams of charged particles could then be measured to determine their relative contributions to the beam current.

Because the cost of developing the concave membranes required for focused beamlets would have been substantial, it was decided that preliminary tests would be conducted using flat membranes. As a result, essentially all of the ions (and electrons) emitted from the membrane struck the accel electrode. The small fraction of these charged particles that passed through the 4.8-mm-diam hole in the accel electrode and could be detected by the mass spectrometer were typically only a few percent of the emission or cathode current (J_C in Fig. 4).

For most of the tests conducted to measure the ion emission current capabilities of membrane assemblies, the cathode and accel power supply voltages were set at -500 and 2000 V, respectively. The membrane temperature was increased from ambient temperatures to 600°C at a rate of 5°C/ min, and data were recorded using LabVIEW. During the first of these tests, both cathode emission J_C and accel collection J_A currents were measured using high-accuracy electrometers. After several tests, however, it was determined that these two currents always agreed within a few percent, and it was decided to measure only the cathode emission current along with membrane temperature, oxygen supply pressure, and in some cases, the ion and electron spectrometer currents.

IV. Experimental Results

Initial tests were conducted using the test configuration shown in Fig. 3 to measure the oxygen flow and ion current that could be drawn through the membrane as functions of the voltage applied across it and its temperature. Typical data obtained from these tests are shown in Figs. 5a and 5b. Figure 5a shows the oxygen flow rate determined from ion current measurements plotted against the anode-to-cathode potential difference applied across the membrane, with membrane temperature as a parameter. These data indicate the following:

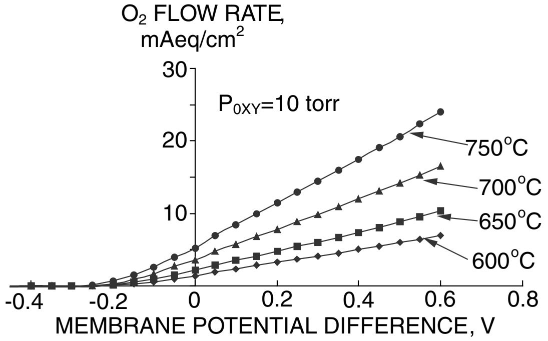

a) Oxygen flow

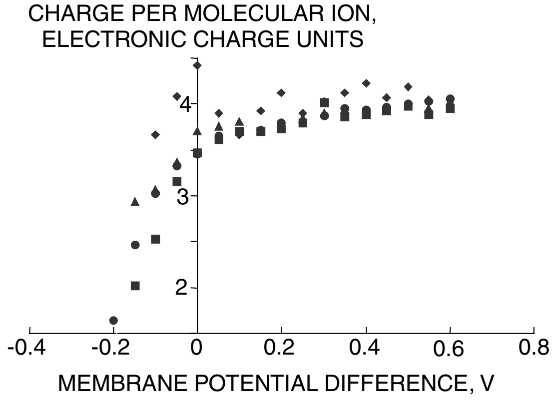

b) Charge per molecular ion

Fig. 5 Membrane performance without high-voltage ion extraction.

1) The ion current increases as the anode is biased more positive relative to the cathode. Hence, the oxygen ions formed at the cathode are negatively charged.

2) Oxygen ions form and flow even when the voltage applied across the membrane is zero or slightly negative. Hence, the modest pressure difference applied across the membrane (10 torr) is sufficient to enable substantial anion formation and diffusion.

3) The rates of oxygen ionization (i.e., electron attachment) at the cathode and flow through the membrane are comparable and possibly greater than those associated with conventional electron-bombardment thrusters (several mA/cm^2) when modest voltages and reasonable temperatures are applied. In this regard, it is noted that solid electrolyte oxygen-separation membranes described by Meixner et al. [4], which are similar to those tested in this study, are typically operated by Ceramatec at about 350 mA/cm^2 for over 35,000 h, with a modest (1%/kh) increase in the required input power. These results, however, do not reflect limitations associated with ion emission from the downstream layer, which would be required in a thrusting device and could therefore degrade its current density, efficiency, and lifetime performance substantially.

The companion data in Fig. 5b enable one to determine the charge state of the oxygen anions that flow through the membrane. The vertical axis values in this plot were obtained by dividing the measured ion current flow through the membrane by the molecular oxygen flow determined from corresponding oxygen partial pressure measurements. Each data point in Fig. 5b corresponds to a data point identified by the same symbol in Fig. 5a. Disregarding the data at potential differences below zero, acknowledging the fact that electron conduction through the membrane should be negligible, and recognizing that the oxygen must migrate in its monatomic state, this plot suggests that each anion that forms at the cathode receives two electrons (four for each anion pair from an oxygen molecule). Hence, the model of the process that evolves for oxygen is that diatomic oxygen dissociates and each resulting oxygen atom (O) receives two electrons as it passes from the cathode layer onto the membrane matrix. It migrates as $O^=$ until it reaches the downstream side of the matrix (anode), to which it gives up its electrons to the anode. Two atomic oxygen atoms are then able to recombine and flow into the vacuum chamber. Ion migration through the matrix is sustained by a combination of the applied electric field and the cathode-to-anode ion concentration gradient. In this experiment, all electrons removed from the ions at the anode flow back to the membrane power supply via the circuit shown in Fig. 3.

To evaluate the overall performance capability of the membrane (i.e., ionization, membrane transmission, and emission/acceleration) the membrane power supply shown in Fig. 3 was removed and high-voltage power supplies in the configuration of Fig. 4 were installed. With the cathode biased to -500 V and the accel electrode biased at 2 kV and positioned 1 mm downstream of the membrane, a 2.5 kV/mm electric field was established at the membrane and negative oxygen ions were extracted into a beamlet. Figure 6 shows that the measured current J_C varied as the membrane temperature was increased from ambient temperatures to 600°C, at a rate of about

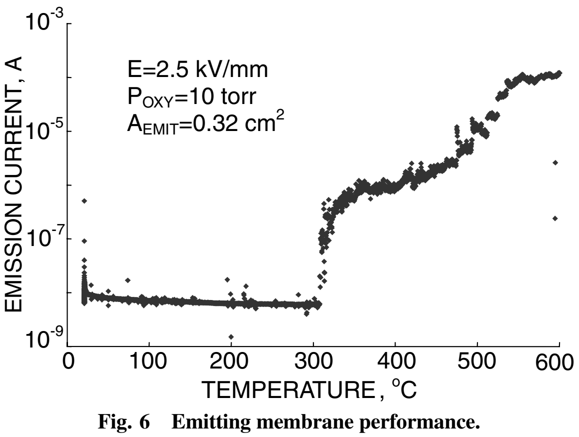

Fig. 6 Emitting membrane performance.

5°C/ min. It shows that currents, which were generally near 10 nA at low temperatures, began to rise near 300°C and reached a maximum over 0.1 mA as 600°C was approached. Because the active membrane area was 0.32 cm^2, this current corresponds to a current density near 0.3 mA/cm^2. This is about an order of magnitude below current densities achieved with ion thrusters for which extraction occurs from a plasma. Considering the preliminary nature of this work and the fact that no steps were taken to enable ready emission from the downstream membrane surface, however, this result is considered to be very promising. It is also noteworthy that researchers working in nonpropulsion applications have reported oxygen ion current emission from ceramic membranes, but the current densities they have achieved are orders of magnitude below the maximum values cited in Fig. 6 [5,6].

It is possible that both negative oxygen ions and electrons are being extracted from the membrane and that the data of Fig. 6 do not represent a pure ion current. The electron content of the beam was investigated by making mass spectroscopic measurements to determine the relative magnitudes of the electron and ion currents. Typical data are shown in Figs. 7a and 7b for the ion and electron currents, respectively. It is argued that these currents are in the nanoamp range, whereas cathode (emission) currents are in the microamp range because of the small fraction of the emission from the flat membrane that passes through the hole in the accel electrode. These figures also show a substantial data scatter that is a reflection of an emission process noisiness that is also evident in Fig. 6. The data of Fig. 7 suggest an electron-to-ion current ratio α near 0.4. For the two reactions that can be expected to yield electrons $[\mathrm{O}^{=} \rightarrow \mathrm{O} + 2\mathrm{e}^{-}$ and $\mathrm{O}^{=} \rightarrow \mathrm{O}^{-} + \mathrm{e}^{-}]$, one finds that the ratio of the actual ion current to its maximum (zero electron emission) value is given by $1/(1+\alpha)$, and so in the case of the data of Fig. 7, this ratio is about 70%. The uncertainty in these data evidenced by the scatter in the data of Figs. 6 and 7 suggests, however, that the values of α are probably no more accurate than ±40%. Still, this corresponds to a measured-to-maximum ion current ratio in the range of 60 to 80%, and so it is argued on the basis of results such as those of Fig. 7 that emission currents shown in Fig. 6 are due primarily to ions. It is further noted that although electron emission is problematic with oxygen ions, it would not be so for the positive propellant ions, which are preferred for an actual thruster application.

The question of why small voltages applied across the membrane yield order-of-magnitude-greater currents (Fig. 5) than one observes when high voltages are imposed between the cathode and the accel electrode (Fig. 6) deserves further consideration. It could be that the membrane is a sufficiently good conductor that the full voltage drop develops between the downstream face of the membrane and the accel electrode and there is no voltage drop through the membrane. This possibility was investigated by measuring the voltage difference across the membrane when the high voltages were applied and ion emission was occurring. Voltage differences were found to be generally similar to those given in Fig. 5a. Hence, it was concluded that it is the emission process occurring on the downstream membrane face that limits the beamlet current.

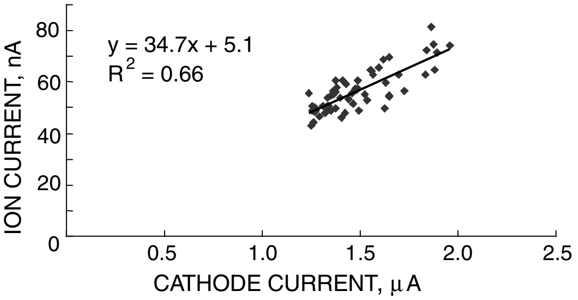

a) Ion measurement

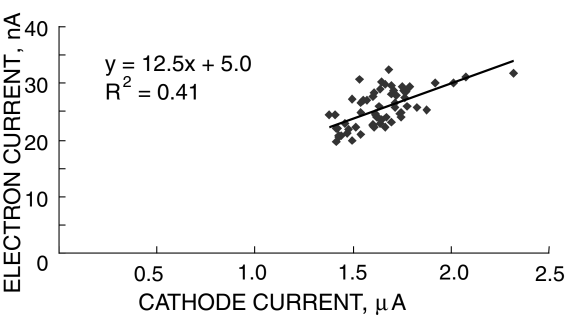

b) Electron measurement

Fig. 7 Typical corresponding mass spectrometer data.

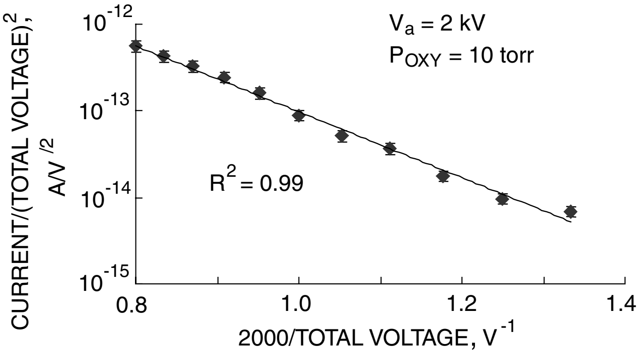

Fig. 8 Fowler–Nordheim plot for oxygen membrane.

The mechanism of ion emission was investigated by varying the high voltage applied to the cathode while holding the accel grid at 2 kV and measuring the associated ion emission current. The most likely emission process for this situation can be expected to be field emission, described by the Fowler–Nordheim equation [7], with the functional form $J_C = CV_T^2 \exp[-a/V_T]$. When the cathode current J_C vs total (cathode-to-accel) voltage difference V_T data were plotted in the rearranged linear form of this equation, the results given in Fig. 8 were obtained. The high degree of linearity of the data in this plot suggests that field emission is the likely mechanism of ion extraction from the surface. This in turn suggests that the ion current density from the device could be improved by reducing the work function for ion emission through proper selection of the downstream membrane material [8].

Other observations from tests such as those that yielded the data of Fig. 6 are that a membrane that had been heated to 600°C and operated tended to exhibit low-temperature ion emission currents near 1 µA rather than 10 nA. This apparent conditioning effect could be beneficial in an actual thruster application. On the other hand, operation for periods of hours at 600°C resulted in a temporal degradation of the ion emission current that could be as great as an order of magnitude per hour. Operation at greater total accelerating voltages induced greater currents than those indicated in Fig. 6, but they also tended to degrade the membrane emission capabilities more rapidly. These degradations are probably related to changes in the emissive surface texture and/or chemistry. They suggest the need for a more durable emissive surface.

V. Emissive Membrane Ion Thruster Conceptualization

The essential features of a module that might be incorporated into an array constituting an emissive membrane ion thruster (EMIT) are shown in Fig. 9. This array would, of course, require a neutralizer to limit adverse space-charge effects. The physical appearance of the module is very similar to that associated with cesium contact ion thrusters developed in the early 1960s [9]. Propellant supplied to the upstream side of the membrane would be ionized and transmitted to the downstream side, from which emission would occur. The membrane surface could be designed and shaped optimally [10] to achieve a desired effect (e.g., maximum beamlet current or minimum beamlet divergence). Because the ionization and transmission processes are surface-defined, the density of ions on the emission surface can be made uniform on this and all other modules of an

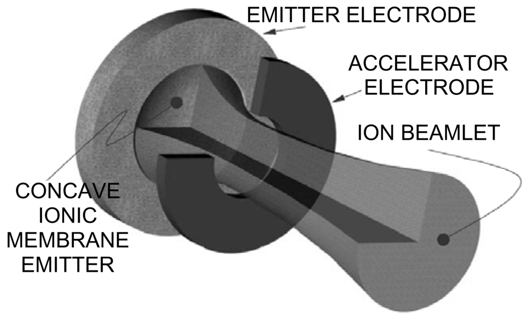

Fig. 9 Emissive membrane ion thruster module.

array. This feature enables a very wide range of scalability on the levels of both the individual modules and the array to achieve desired thrust levels and specific impulses.

As mentioned previously, good ionic conduction has been observed with many elements (e.g., silver and bismuth) from which a preferred propellant could be selected. Essentially all of those elements but oxygen produce positive ions, and this desirable feature plus a preference for a heavy ion leads one away from oxygen for most thruster applications. It is noted that the propellant can be a gas, a liquid, or even a solid. In the latter case, some solids could be used directly and others could be transported as particles in a liquid carrier. The carrier approach is viable because the membranes are selective, and so only the solid particle atoms would be ionized and transported through them. In this regard, it is noted that potential contaminants such as the transport liquid and extraneous molecules generally do not affect the performance of ionic conductors unless they accumulate to the point at which they block access of the active element atoms to the membrane.

The data of Fig. 5 show that ions can be produced at a very low energy cost per ion. One can expect that the energy cost of propellants other than oxygen would be similar to the values of Fig. 5 ($O^{=}$ ionization and transmission costs would be less than twice the maximum membrane potential difference; that is, 1.2 eV/ion). To this, one would add the work function (a few electron volts) required for emission and the energy per ion radiated from each hot emitter surface. The operating temperature required for a cesium contact thruster was between 1100 and 1200°C, and as a result, it had high thermal radiation losses [9] and this led to its demise. The operating temperatures shown in Figs. 5a and 6 are substantially lower and they will yield much lower radiated powers per unit area. When divided by a corresponding ion current density, these radiated powers per unit area yield radiative-loss contributions to the beam ion energy costs. If one assumes that Fig. 5 current densities and a membrane radiative emissivity of 0.5 could be realized, then the beam ion energy costs plotted in Fig. 10 are obtained. It is noteworthy that energy cost drops as temperature increases over the indicated range, because current density increases more rapidly with temperature than does radiated power per unit area. The beam ion energy costs in Fig. 10 are less than those for state-of-the-art electron-bombardment thrusters, and this implies that energy efficiencies of the EMIT should be greater than those for conventional thrusters.

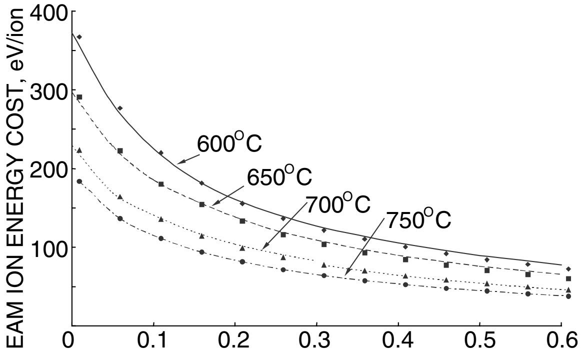

Fig. 10 Beam ion energy cost estimate considering radiation losses.

Propellant use efficiency is probably even more important than energy efficiency, because it affects specific impulse, charge-exchange ion production (hence thruster lifetime), and overall thruster efficiency. Typical discharge values for electron-bombardment thrusters are near 90%. For the cesium contact thruster, the corresponding membrane values were closer to 98%, and for the EMIT, the corresponding membrane use efficiencies should be even greater. Assuming that positive ions would be used, no electron emission should occur. This, coupled with the fact that neutral atoms would not be conducted through these selective membranes, suggests that thruster propellant use efficiencies approaching 100% can be expected.

VI. Comparison with State-of-the-Art Ion Thrusters

Comparison of key features of EMIT with those of a bombardment thruster such as those of the xenon ion propulsion system (XIPS) class suggests that EMIT would enable the following:

1) Elimination of the discharge chamber, including magnets, a hollow cathode, and the discharge power supply.

2) Mitigation of grid-shorting concerns, because there would be no metal flakes generated from films of sputter-eroded material. In addition, because each module operates at the same efficiency and current, there is no need to use large-diameter grid sets that can deflect and distort significantly.

3) Substantially greater membrane propellant use and power efficiencies, even with modest reductions, reflecting the effects of neutralizer propellant and power losses.

4) Operation at higher current densities and therefore higher thrust densities over a wider range of specific impulses, enabled by the flexibility to shape the membrane emissive surface [10] and also by the fact that neutral propellant losses should be negligible.

5) Elimination of the flow-regulation portion of the propellant feed system on the basis of tests reported herein, which have shown that it is necessary only to maintain a modest pressure on each membrane to effect its independent operation. The membranes automatically draw the propellant atoms they need to replace ions that have been ionized and extracted. If throttling were required, it could be accomplished with a small number of valves to stop flow to zones in the array or possibly by reducing membrane temperatures. It is noted that combinations of three valves that would stop individual flows to 10, 20, and 30% of an array would enable thrust levels from 100 to 40% in 10% increments.

6) Simplification of fabrication enabled by laminated-object manufacturing techniques with their potential for great cost savings and capacity to make lightweight EMIT arrays with modules of various sizes containing integrated flow passages and, if desired, conducting ceramic accel electrodes.

The system consequences of using EMIT as suggested by the preceding list are substantial. They include 1) lower system cost, mass, and complexity; 2) greater system reliability and failure tolerance; and 3) higher thrust-to-power capabilities, especially at low specific impulses. These system features, which are greatly enhanced by scalability from multimeter to nanometer dimensions without efficiency degradation, also mean that the emissive membrane ion thruster technology is particularly well suited to microthruster applications.

There are also significant challenges associated with the development of an emissive membrane ion thruster. Although some experience has been gained in the field emission of ions in the field emission electric propulsion (FEEP) class of thrusters [11], effective implementation of this process is considered to be the greatest challenge associated with EMIT development. Problems associated with this process are likely to manifest themselves as limitations on thruster lifetime. Even if low-work-function ion-emissive coatings that will enable high-current-density ion emission can be developed, they can be expected to degrade with time. The degradation will be enhanced by the effects of surface contamination and possibly sputter erosion of the coating. In addition, the lack of experience with thin ceramic membranes in propulsion applications is likely to result in unforeseeable challenges.

VII. Conclusions

Solid-state ionic conductors formed into membranes have properties that enable them to ionize propellant atoms at an upstream surface and transport them to a downstream surface, from which they can be extracted by an electric field and formed into an ion beamlet. The processes of ionization and transport through the membrane are very efficient and yield current densities that are as great or greater than those achieved in conventional electron-bombardment ion thrusters. The field emission process limits the current density of ions that can actually be extracted from ionic conductor surfaces that have not been treated to effect a low work function for the emission of ions. There are many features of the emissive membrane ion thruster that make it an attractive competitor to conventional ion thruster technology.

Acknowledgments

Funding from the NASA John H. Glenn Research Center at Lewis Field under Phase 1 Small Business Innovative Research contract no. 03-S1.02-8120 supported a portion of this work. That funding and the careful work of Jeff Kawola, who assisted in the preparation of the membranes, are gratefully acknowledged.

References

[1] Cybulski, R. J., Shellhammer, D. M., Lovell, R. R., Domino, E. J., and Kotnik, J. T., "Results from SERT 1 Ion Rocket Flight Test," NASA TN D-2718, Mar. 1965.

[2] Brophy, J., "Advanced Ion Propulsion Systems for Affordable Deep-Space Missions," *Acta Astronautica*, Vol. 52, Nos. 2–6, 2003, pp. 309–316.

[3] Knauth, P., and Tuller, H. L., "Solid State Ionics: Roots, Status, and Future Prospects," *Journal of the American Ceramic Society*, Vol. 85, No. 7, 2002, pp. 1654–80.

[4] Meixner, D. L., Brengel, D. D., Henderson, B. T., Abardo, J. M., Wilson, M. A., Taylor, D. M., and Cutler, R. A., "Electrochemical Oxygen Separation Using Solid Electrolyte Ion Transport Membranes," *Journal of the Electrochemical Society*, Vol. 149, No. 9, 2002, pp. D132–D136.

[5] Li, Q., Hayaski, K., Nishioka, M., Hashiwagi, H., Hirano, M., Torimoto, Y., Hosono, H., and Sadakata, M., "Absolute Emission Current Density of O^- from $12CaO\ 7Al_2O_3$ crystal," *Applied Physics Letters*, Vol. 80, No. 22, 2003, pp. 100–112.

[6] Fujiwara, Y., Kaimai, A., Hong, J.-O., Yashiro, K., Nigara, Y., Kawada, T., and Mizusaki, J., "An Oxygen Negative Ion Source of a New Concept Using Solid Oxide Electrolytes," *Journal of the Electrochemical Society*, Vol 150, No. 2, 2003, pp. E117–E124.

[7] Fowler, R. H., and Nordheim, L., "Electron Emission in Intense Electric Fields," *Proceedings of the Royal Society of London, Series A: Mathematical and Physical Sciences*, Vol. 119, No. 781, 1928, pp. 173–181.

[8] Kawano, H., Kenpo, T., Koga, H., and Hidaka, Y., "Evaluation of the Effective Work Functions of a Binary Salt Using Thermochemical Data on its Two Constituent Elements," *International Journal of Mass Spectrometry and Ion Physics*, Vol. 52, Nos. 2–3, 1983, pp. 241–246.

[9] Brewer, G. R., *Ion Propulsion*, Gordon and Breach, New York, 1970, pp. 102–127.

[10] Wilbur, P. J., Farnell, C. C., and Williams, J. D., "Ion Thruster Optical Performance Enhancement via Ion Emissive Surface Shaping," 29th International Electric Propulsion Conference, Princeton, NJ, Electric Rocket Propulsion Society Paper 2005-95, 2005.

[11] Tajmar, M., Genovese, A., and Steiger, W., "Indium Field Emission Electric Propulsion Microthruster Experimental Characterization," *Journal of Propulsion and Power*, Vol. 20, No. 2, 2004, pp. 211–218.

R. Myers
Associate Editor